

## Legends to Supplementary Tables and Figures

**Supplementary Table S1.** The source data underlying each of the figure panels, including: the values plotted in graphs, the exact p-values, and the uncropped blots.

**Supplementary Figure S1. Impact of PARP14 on cell cycle progression.** **A.** Left: Western blots showing the levels of PARP14 upon transfection of RPE-1 cells with reduced amounts (5nM and 10nM final concentrations) of PARP14 siRNA. Right: Quantifications showing the percent of RPE-1 cells in G1 cell cycle phase upon PARP14 knockdown using 5nM and 10nM siRNA concentrations. IPO11 knockdown was used as an additional negative control. Bars represent the means  $\pm$  SEM (*t*-test, unpaired). **B.** Quantification showing the percent of RPE-1 cells in G1 cell cycle phase upon PARP14 knockdown and subsequent treatment with 9 $\mu$ M RO-3306 for 24h. Bars represent the means  $\pm$  SEM (*t*-test, unpaired). **C.** Cell cycle profiles of BJ cells upon PARP14 knockdown and subsequent treatment with 200ng/mL nocodazole for 24h. **D.** Quantification showing the percent of BJ cells in G1 cell cycle phase upon PARP14 knockdown and subsequent treatment with 200ng/mL nocodazole for 24h. Bars represent the means  $\pm$  SEM (*t*-test, unpaired). Western blots showing PARP14 depletion by siRNA in BJ cells are also presented. **E.** Quantification showing the percent of Annexin-V positive RPE-1 cells upon PARP14 knockdown. Bars represent the means  $\pm$  SEM (*t*-test, unpaired). **F, G.** Western blots showing PARP14 depletion by siRNA in HCT116 (**F**) and MCF7 (**G**) cells. **H.** Proliferation assay in MCF7 cells showing the impact of PARP14 knockdown. Bars represent the means  $\pm$  SEM (*t*-test, unpaired). **I.** Western blots showing PARP14 depletion by siRNA in HCC1395 cells. **J.** Cell cycle profiles of HCC1395 cells upon PARP14 knockdown and subsequent treatment with 100ng/mL nocodazole for 24h. **K.** Quantification showing the percent of HCC1395 cells in G1 cell cycle phase upon PARP14 knockdown and subsequent treatment with 100ng/mL nocodazole for 24h. Bars represent the means  $\pm$  SEM (*t*-test, unpaired).

**Supplementary Figure S2. Impact of PARP14 on RB.** **A.** Quantifications of western blots showing the levels of total RB and of phosphorylated RB at Ser780 upon PARP14 knockdown in RPE-1 cells. Bars represent the means  $\pm$  SEM (*t*-test, unpaired) from three independent experiments. **B.** Western blots showing the levels of phosphorylated RB at Ser780 upon PARP14 knockdown in MCF7 cells. Also shown are quantifications of western blots showing the levels of phosphorylated RB at Ser780 upon PARP14 knockdown in MCF7 cells. Bars represent the means  $\pm$  SEM (*t*-test, unpaired) from three independent experiments. **C.** Quantifications of western blots showing the levels of phosphorylated RB at Ser780 upon PARP14 knockdown in HCT116 cells. Bars represent the means from two independent experiments. **D.** Western blots showing the levels of phosphorylated RB at Ser780 upon PARP14 knockdown in HCC1395 cells. Also shown are quantifications of western blots showing the levels of phosphorylated RB at Ser780 upon PARP14 knockdown in HCC1395 cells. Bars represent the means  $\pm$  SEM (*t*-test, unpaired) from three independent experiments. **E.** Quantifications of western blots showing the levels of E2F1 upon PARP14 knockdown in RPE-1 cells. Bars represent the means  $\pm$  SEM (*t*-test, unpaired) from three independent experiments. **F.** Quantifications of western blots showing the levels Cyclin A, Cdc6, Cyclin B1, and Chk1 upon PARP14 knockdown in RPE-1 cells. Bars represent the means  $\pm$  SEM (*t*-test, unpaired) from three independent experiments for Cyclin A and Cdc6, and the means from two independent experiments for Cyclin B1 and Chk1. **G.** Western blots showing the RB knockout in RPE-1 cells. **H.** Quantification showing the percent of RPE-1 WT and RB<sup>KO</sup> cells in G2/M cell cycle phase upon PARP14 knockdown and subsequent treatment with 200ng/mL nocodazole for 24h. Bars represent the means  $\pm$  SEM (*t*-test, unpaired). Western blots showing the PARP14 levels upon PARP14 depletion by siRNA in these cells are also presented. **I.** Western blots showing the PARP14 levels upon PARP14 depletion by siRNA in palbociclib-resistant T47D cells (T47D-R). **J.** Cell cycle profiles of RPE-1 RB<sup>KO</sup> cells upon PARP14 knockdown and p107 co-depletion, and subsequent treatment with

200ng/mL nocodazole for 24h. **K.** Quantification showing the percent of RPE-1 RB<sup>KO</sup> cells upon PARP14 knockdown and p107 co-depletion, and subsequent treatment with 200ng/mL nocodazole for 24h. Bars represent the means  $\pm$  SEM (*t*-test, unpaired). Western blots showing p107 depletion are also presented. **L.** Western blots showing PARP14 depletion by siRNA in RPE-1 WT and RB/p107/p130 TKO cells.

**Supplementary Figure S3. Loss of p53 partially rescues G1 arrest upon PARP14**

**depletion in HCT116 cells.** **A.** Western blots showing the p53 knockout in RPE-1 cells. **B.** Cell cycle profiles of HCT116 WT and p53<sup>KO</sup> cells upon PARP14 knockdown. **C.** Quantification showing the percent of HCT116 WT and p53<sup>KO</sup> cells in G1 cell cycle phase upon PARP14 knockdown. Bars represent the means  $\pm$  SEM (*t*-test, unpaired). **D.** Quantifications of western blots showing the levels of phosphorylated RB at Ser780 upon PARP14 knockdown and p21 co-depletion in RPE-1 cells. Bars represent the means from two independent experiments.

**Supplementary Figure S4. Impact of PARP14 on Cyclin D1 expression, AKT, and ERK**

**signaling.** **A.** Quantifications of western blots showing the levels Cyclin D1 upon PARP14 knockdown in RPE-1, MCF7, and HeLa cells. Bars represent the means  $\pm$  SEM (*t*-test, unpaired) from three independent experiments for RPE-1 and HeLa, and the means from two independent experiments for MCF7. **B.** Western blots showing Cyclin D1 levels upon PARP14 knockdown in RPE-1 RB/p107/p130 TKO cells. **C.** Western blots showing PARP14 knockout in HeLa, MCF7 and RPE-1 RB/p107/p130 TKO cells. **D.** Western blots showing Cyclin D1 levels upon PARP14 knockdown in RPE-1 cyclin D1-overexpressing cells. **E.** Quantification showing the percent of RPE-1 WT and cyclin D1-overexpressing cells in G2/M cell cycle phase upon PARP14 knockdown and subsequent treatment with 200ng/mL nocodazole for 24h. Bars represent the means  $\pm$  SEM (*t*-test, unpaired). Western blots showing the PARP14 levels upon PARP14 depletion by siRNA in these cells are also presented. **F.** Quantifications of western

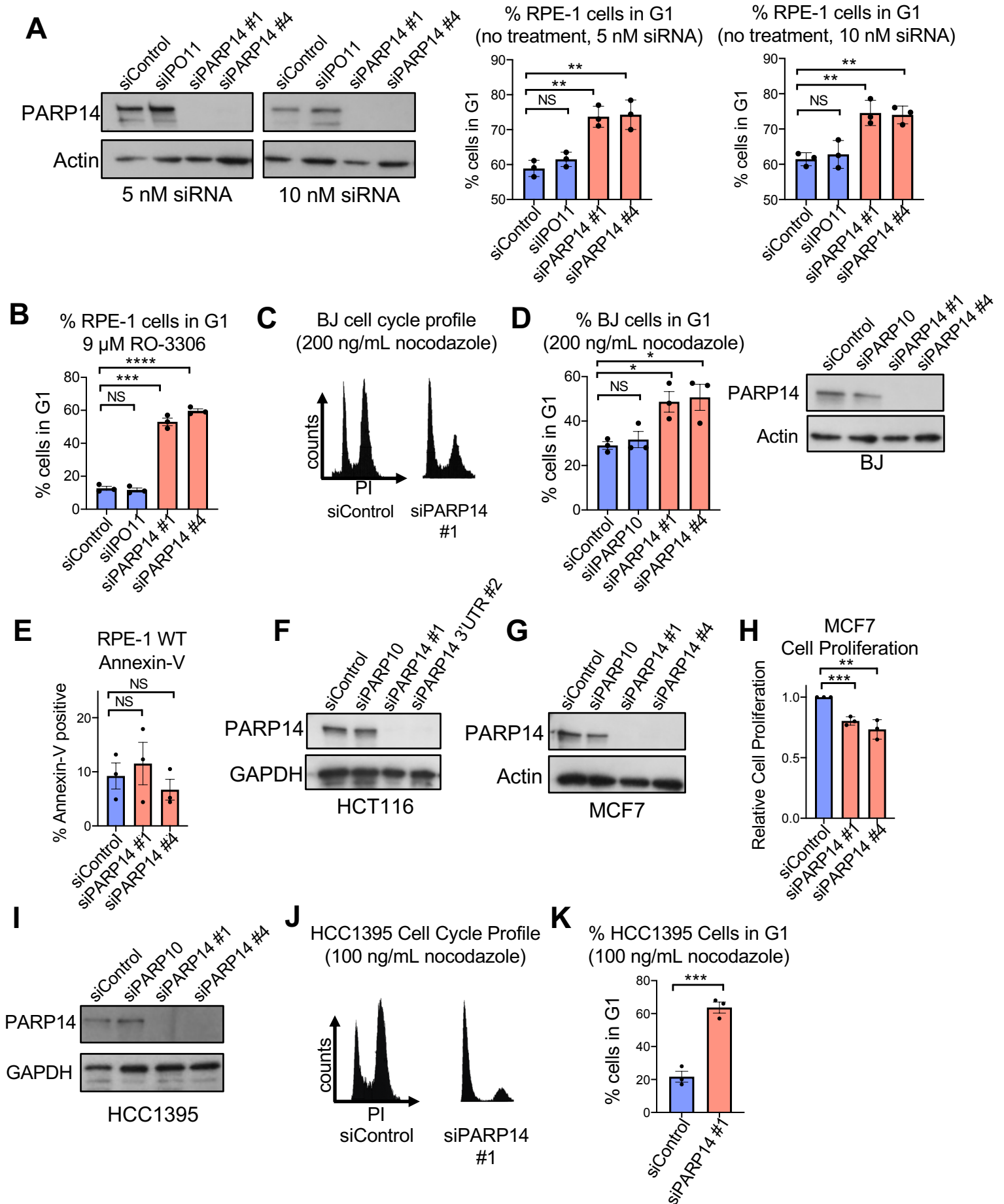
blots showing the levels of phosphorylated RB at Ser780, E2F1, and Cdc6 upon PARP14 knockdown in wildtype and Cyclin D1-overexpressing RPE-1 cells. Bars represent the means  $\pm$  SEM (*t*-test, unpaired) from three independent experiments. **G.** Quantifications of western blots showing the levels of phosphorylated RB at Ser780 from *in vitro* kinase assays using recombinant RB as a substrate and Cyclin D1/CDK4 kinase complexes immunoprecipitated from RPE-1 WT or cyclin D1- overexpressing cells upon PARP14 knockdown. Bars represent the means from two independent experiments. **H.** Western blots showing the levels of ERK1/2 and phosphorylated ERK1/2 upon PARP14 knockdown in RPE-1 cells. **I.** Western blots showing the levels of Akt and phosphorylated Akt at Ser473 upon PARP14 knockdown in RPE-1 cells.

**Supplementary Figure S5. Loss of p53 rescues the G1 arrest caused by PARP14**

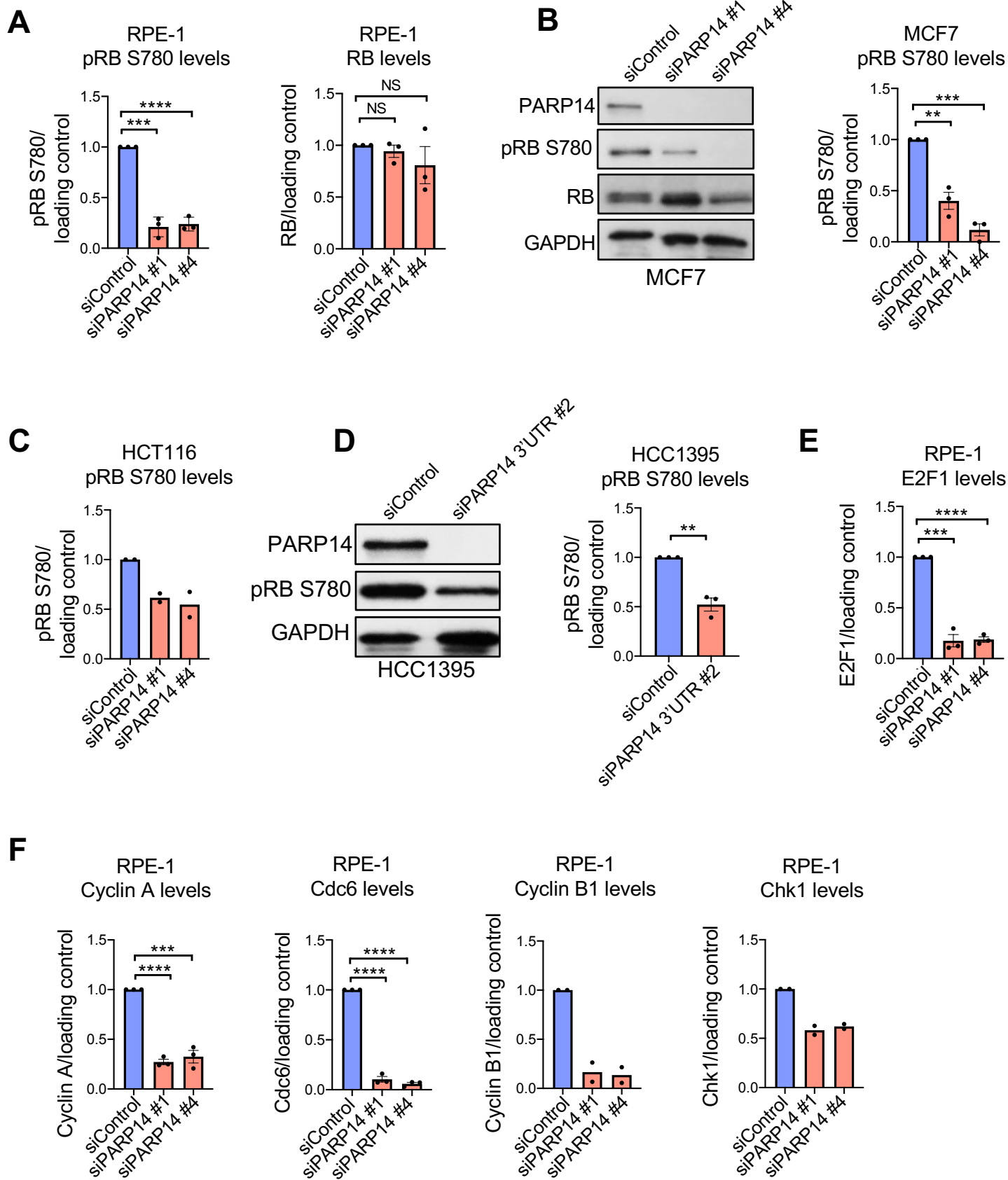
**knockdown in cyclin D1-overexpressing cells. A.** Quantification showing the percent of RPE-1 cyclin D1-overexpressing cells in G2/M cell cycle phase upon PARP14 knockdown and p53 co-depletion, and subsequent treatment with 200ng/mL nocodazole for 24h. Bars represent the means  $\pm$  SEM (*t*-test, unpaired). **B.** Western blots showing the levels of phosphorylated RB at Ser780 in RPE-1 cyclin D1- overexpressing cells upon PARP14 knockdown and p53 co-depletion.

**Supplementary Figure S6. Schematic depiction of the proposed model.** PARP14 promotes the 3'UTR stability of the cyclin D1 mRNA. In its absence, cyclin D1 levels are reduced and RB phosphorylation is impaired, resulting in G1 arrest. (Created with Biorender.com)

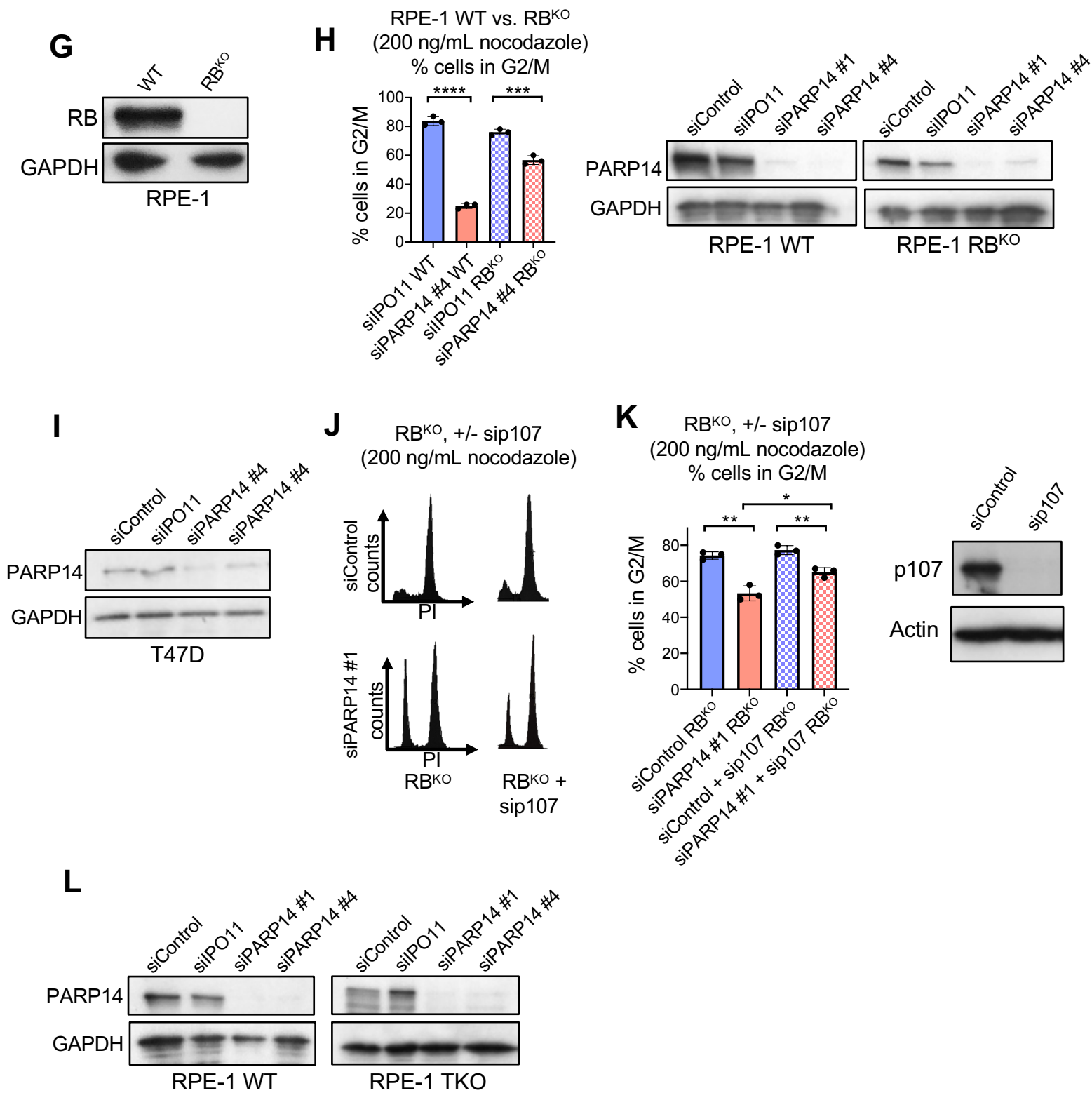
# Supplementary Figure S1



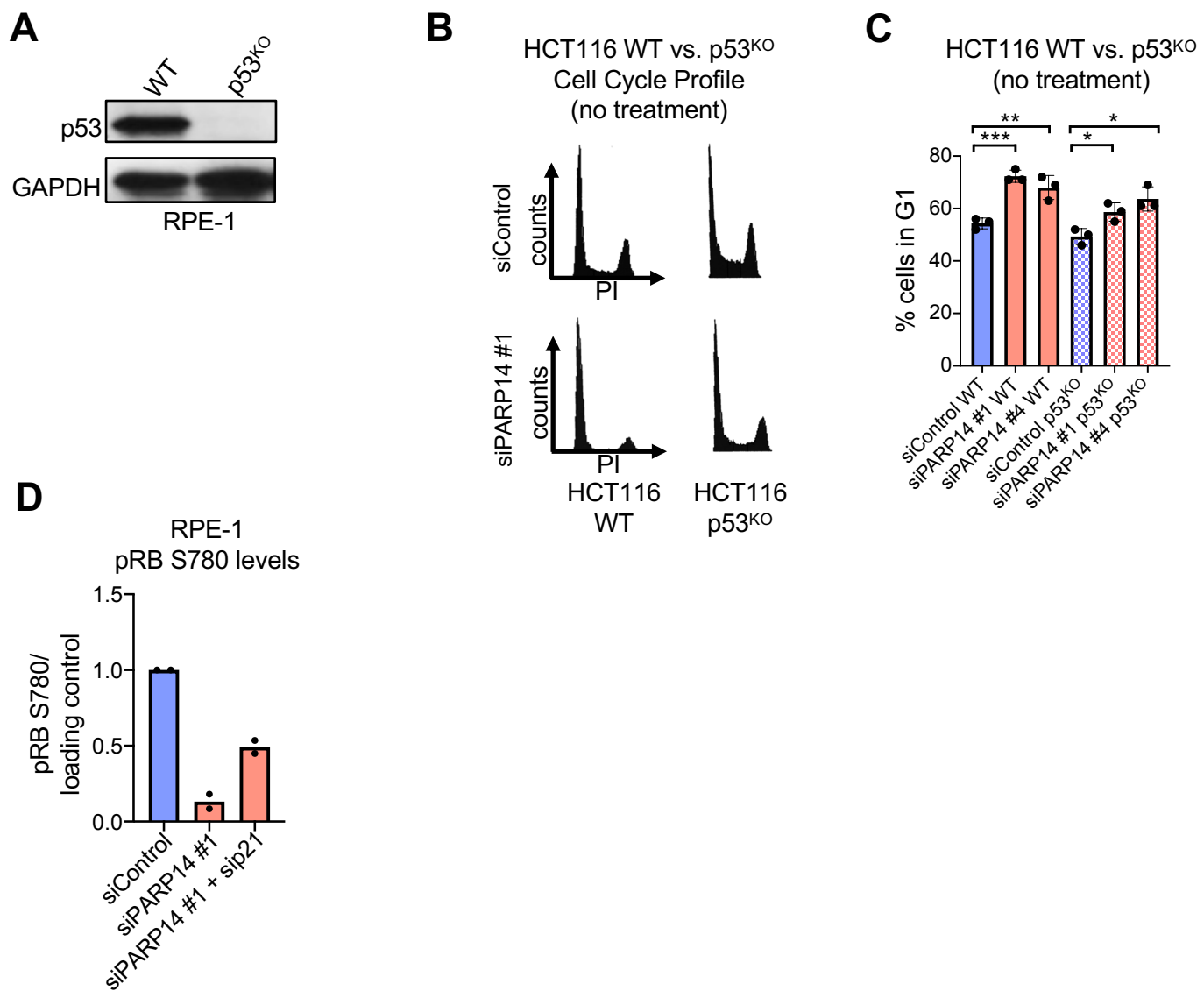
# Supplementary Figure S2



## Supplementary Figure S2 (continued)

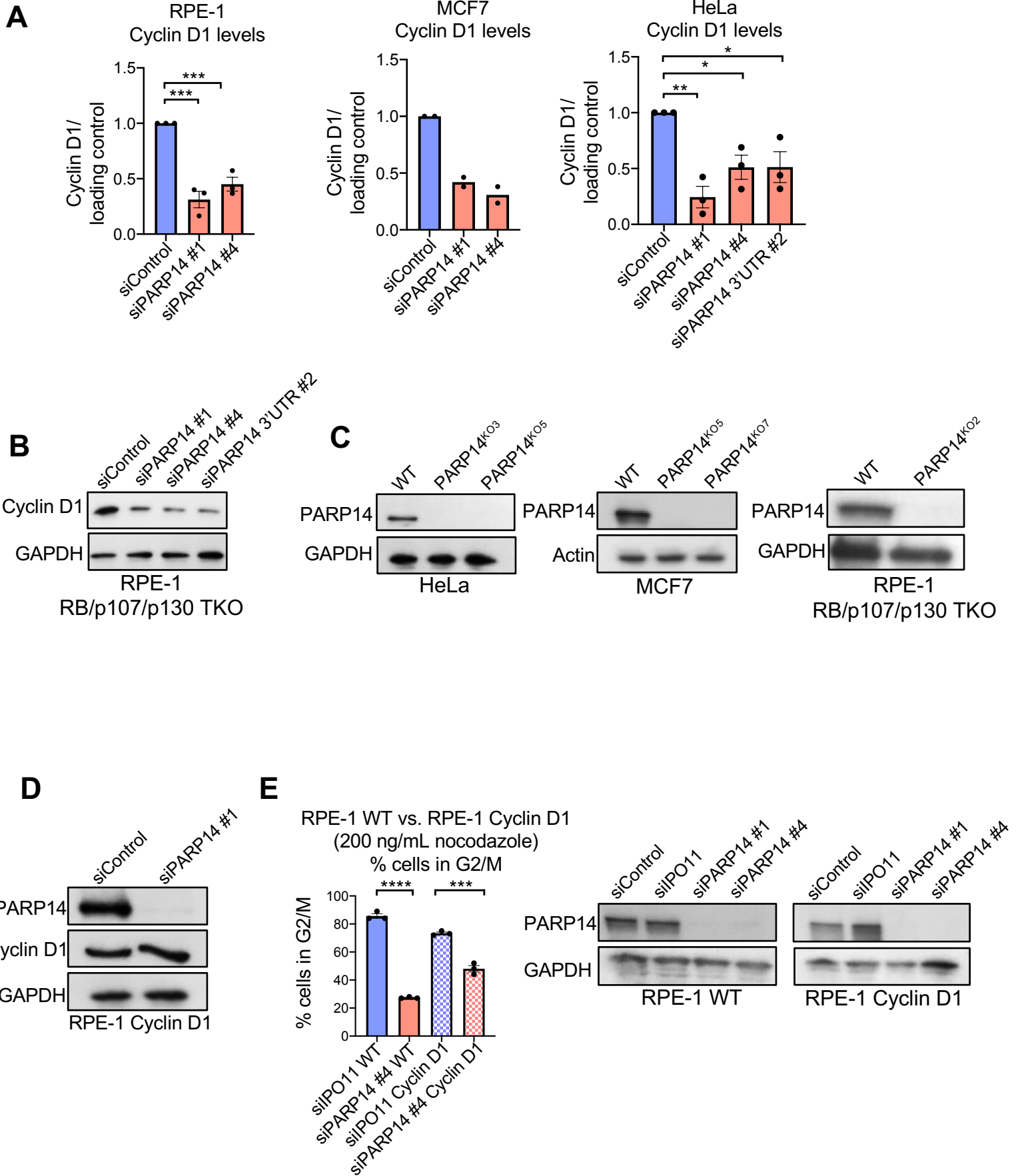


# Supplementary Figure S3

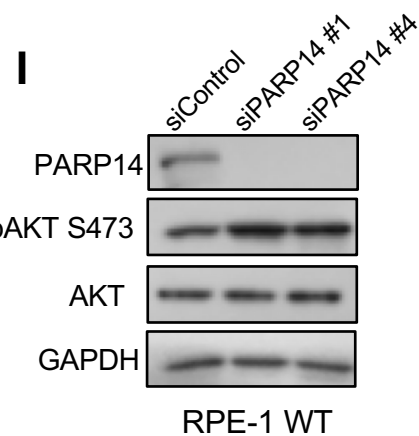
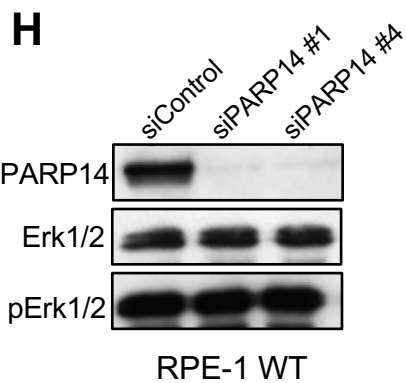
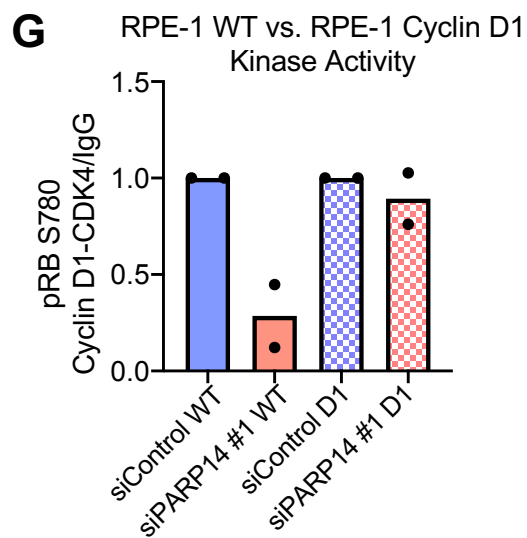
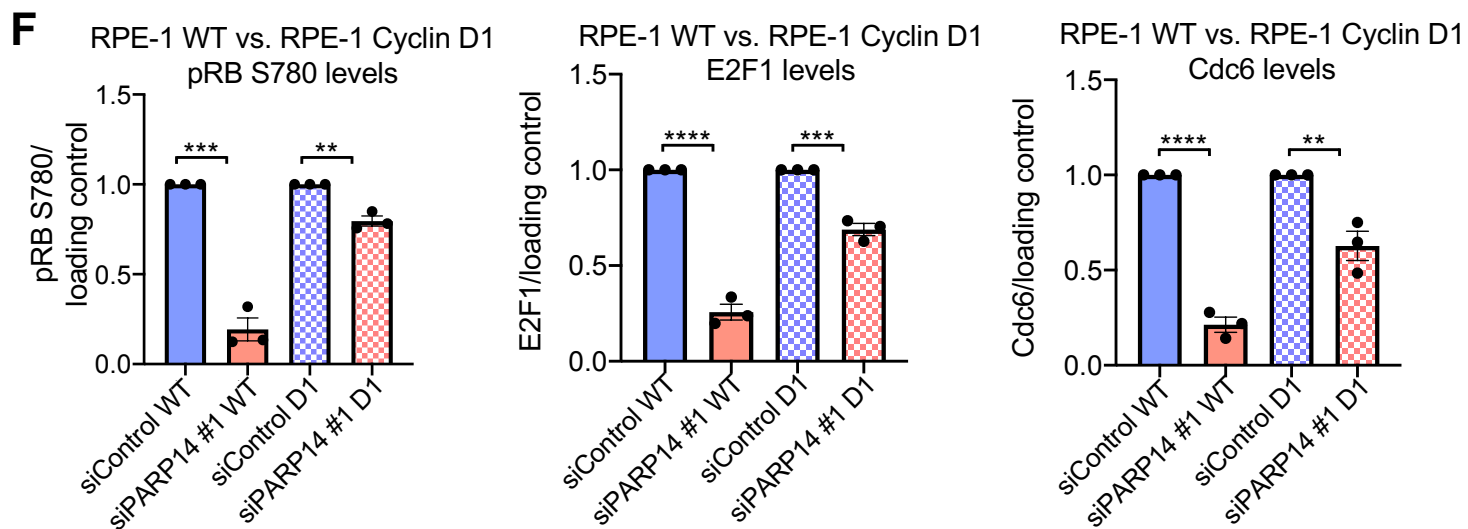




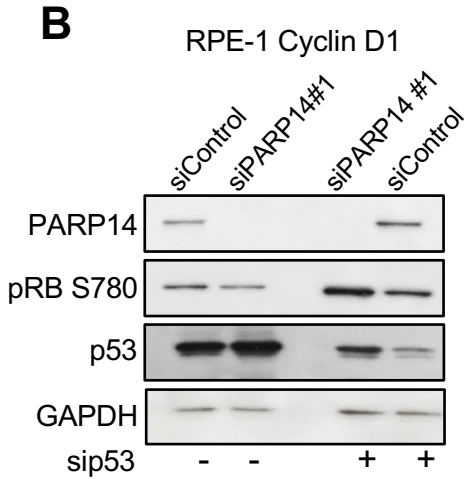
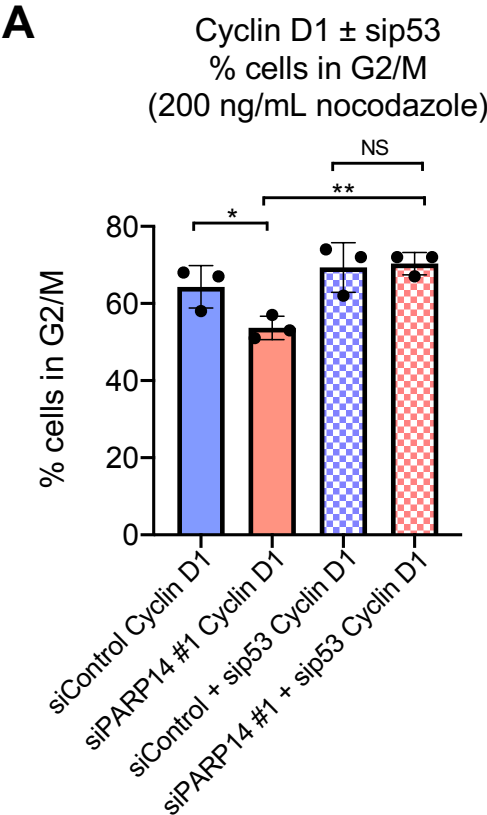
# Supplementary Figure S4



# Supplementary Figure S4 (continued)



# Supplementary Figure S5



# Supplementary Figure S6

## PARP14 regulates cyclin D1 mRNA stability

